Electronic Supplementary Material (ESI) for Journal of Materials Chemistry C.

Unusual structural-disorder stability of mechanochemically derived-$Pb(Sc_{0.5}Nb_{0.5})O_3$ ceramics

Hana Uršič,[a] Andreja Benčan,[a] Goran Dražič,[a,b] Giovanni Esteves,[c] Jacob L. Jones,[c] Tedi-Marie Usher,[c] Tadej Rojac,[a] Silvo Drnovšek,[a] Marco Deluca,[d,e] Jenny Jouin,[f] Vid Bobnar,[a] Gregor Trefalt,[a+] Janez Holc,[a] Barbara Malič[a]

[a]Jožef Stefan Institute, Jamova cesta 39, Ljubljana, Slovenia

[b]Laboratory for Materials Chemistry, National Institute of Chemistry, Ljubljana, Slovenia

[c]Department of Materials Science and Engineering, North Carolina State University, Raleigh, NC, USA

[d]Institut für Struktur- und Funktionskeramik, Montanuniversitaet Leoben, Peter Tunner Str. 5, Leoben, Austria

[e]Materials Center Leoben Forschung GmbH Roseggerstr. 12, Leoben, Austria

[f]Science des Procédés Céramiques et de Traitements de Surface, Centre Européen de la Céramique, 12 rue Atlantis, Limoges Cedex, France

+ current address: University of Geneva, Switzerland

A) Literature data

Table S1: Preparation conditions for disordered and ordered PSN ceramics as reported by different groups.

ref.	Thermal treatment	Packing powder	B-site ordering
[S1]	**1430 °C**, 20 min, quenched	yes	disordered
[S2]	**1420 °C**, 15 min , quenched	yes	disordered
[S3]	**1300 °C**, 2 h, cooled	/	disordered
[S4]	**1250 °C**, 8 h in O_2, cooled	yes	disordered
[S5]	**1210 °C**, 2 h, quenched	/	disordered
[S6]	ordered sample was annealed at **1210 °C**, /	yes	disordered
[S5]	**1000 °C**, **24 days**	/	ordered
[S3]	disordered samples (1300 °C, 2 h) were annealed at **1000 °C**, **50 h**	/	ordered
[S1]	1250 °C, 4 h, annealed at **1000 °C, 42 h**	yes	ordered
[S7]	1250 °C, 4 h, annealed at **1000 °C**, **42 h**	yes	ordered
[S6]	**950 °C**, **2 h**	/	ordered
[S4]	**940 °C**, **1 month**	yes	ordered

B) Details of MA-derived PSN powder

The reagent powder mixture after 24 h of mechanochemical activation consists of the perovskite PSN phase and the initial oxides PbO, Sc_2O_3 and Nb_2O_5 as well as a small amount of the amorphous phase as evident from the XRD spectrum in Fig. S1(a). Note that the diffraction peaks are quite broad, indicating low crystallinity of the powder. After heating of the mechanochemically activated powder mixture at 800 °C for 1 h the XRD pattern evidences a well crystallized perovskite phase, see Fig. S1(b). No traces of secondary phases, such as pyrochlore or PbO, could be detected.

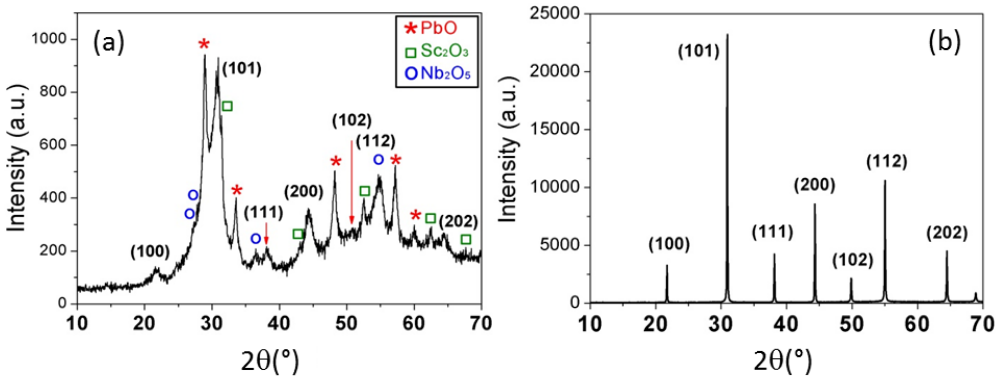

Fig. S1: The XRD pattern of the PSN powder (a) after mechanochemical activation and (b) after heating at 800 °C for 1 h. The indexed peaks of the perovskite phase are shown in brackets (ICSD #80922).

In Fig. S2, the FE-SEM micrograph and the particle size distribution of the powder after the mechanochemical activation, heating and additional milling in an attrition mill are shown. The powder is uniform, consisting of particles of a few 100 nm sized particles. According to the granulometric analysis the particle size distribution is unimodal, with the median size d_{50} and the d_{90} equal to 385 nm and 890 nm, respectively.

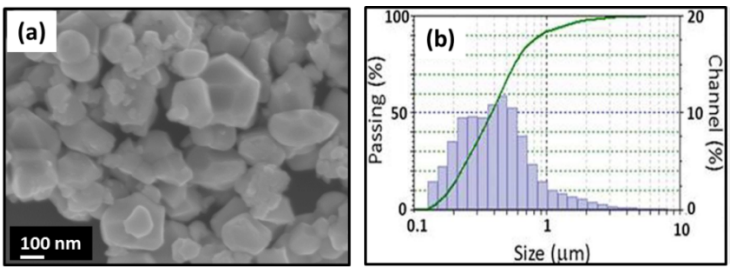

Fig. S2: (a) The FE-SEM micrograph and (b) the particle area size distribution of the PSN powder after mechanochemical activation, heating at 800 °C for 1h, and attrition milling.

C) SS-derived PSN powder and ceramics

For the synthesis of the $Pb(Sc_{0.5}Nb_{0.5})O_3$ (PSN) powder by SS-synthesis, PbO (99.9%, Sigma-Aldrich, 211907), Sc_2O_3 (99.9% Alfa Aesar, 11216) and Nb_2O_5 (99.9%, Sigma-Aldrich, 208515) were used as raw materials. The mixture of Sc_2O_3 and Nb_2O_5 was homogenized in a planetary mill for 2 h at 200 rpm. The powder was then heated on a Pt foil in an alumina crucible at 1280 °C for 4 h at 5 °C/min. The PbO was added into the powder mixture and the powder was homogenized for 2 h in a planetary mill. The homogenized powder was than heated at 1000 °C for 4 h. The powder compacts were prepared by isostatic pressing at 300 MPa and sintered in double alumina crucibles in the packing powder with the same chemical composition to avoid possible PbO losses. Different thermal treatments of the PSN powder compacts were employed. As we can see from Table 1 (main text), the *SS1200* ceramics were heated at T_{OD}, while other samples were exposed to lower temperatures. The densities of the sintered pellets were determined with the Archimedes' method in water at 25 °C. The density of all samples was between 92-94 % of the theoretical density (TD), which is lower than the density of MA-derived samples, i.e., 99 % of TD (main text, results and discussion). It is well known from the literature that pores may inhibit the grain growth during sintering [S8]. Thus, the lower grain size of the SS-derived ceramics might be related to the higher porosity in this sample (relative to the MA-derived ceramics), which prevented a full development of the microstructure through grain growth.

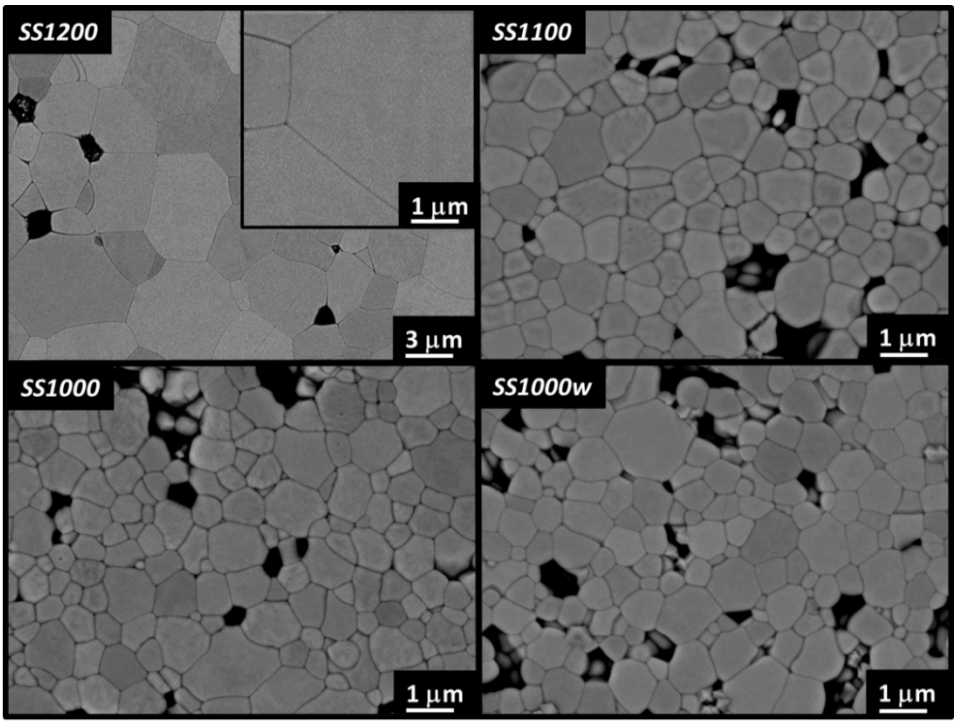

Fig. S3: FE-SEM micrographs of the thermally etched PSN ceramics, prepared by SS synthesis as described in Table 1 (main text). The microstructures are uniform. No secondary-phases could be detected.

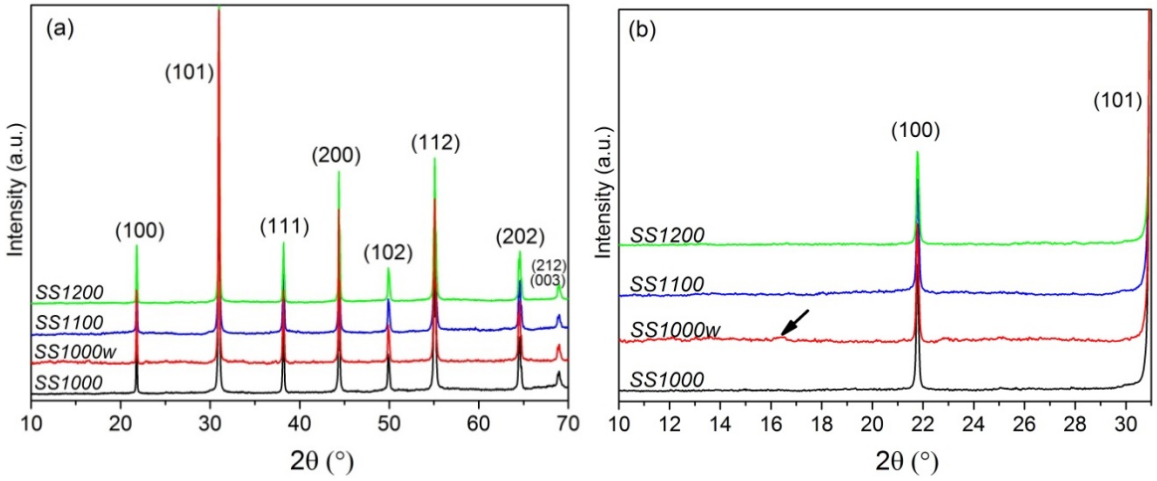

Fig. S4: (a) Room-temperature XRD patterns of the PSN ceramics prepared by SS synthesis exposed to different thermal treatments as described in Table 1 (main text). The indexed peaks of the perovskite phase are shown in brackets (ICSD #80922). (b) Zoom of the XRD patterns from 10 to 33° showing that there are no superstructure peaks, except small peak in pattern of *SS1000w*, which could be related to the superstructure.

D) Phase composition of MA-derived PSN ceramics

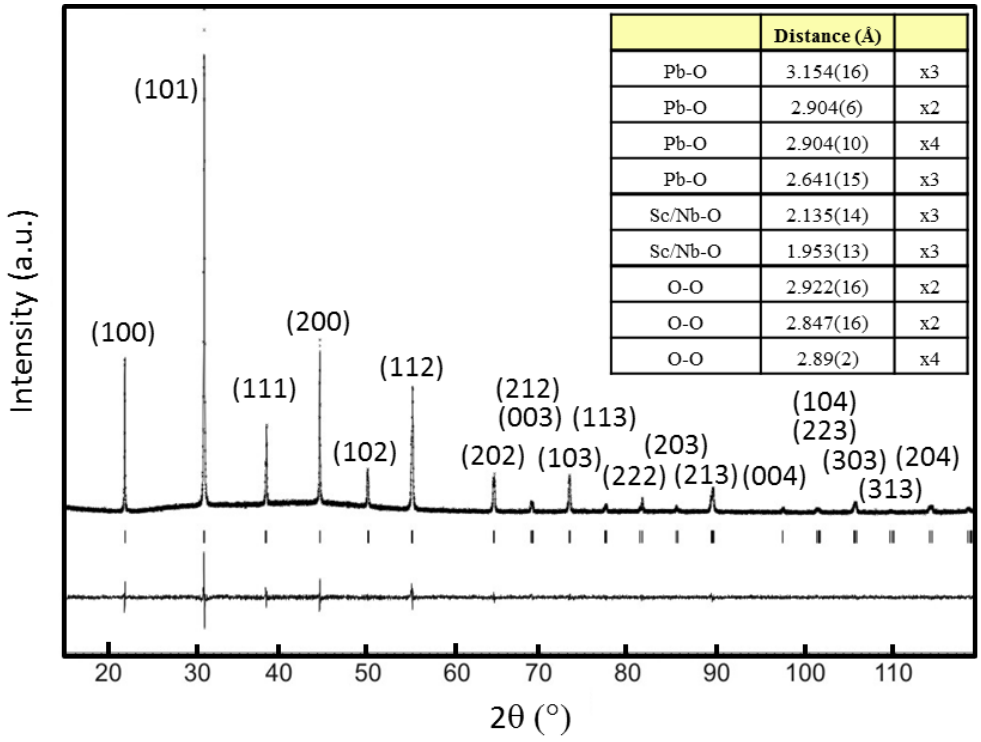

	Distance (Å)	
Pb-O	3.154(16)	x3
Pb-O	2.904(6)	x2
Pb-O	2.904(10)	x4
Pb-O	2.641(15)	x3
Sc/Nb-O	2.135(14)	x3
Sc/Nb-O	1.953(13)	x3
O-O	2.922(16)	x2
O-O	2.847(16)	x2
O-O	2.89(2)	x4

Fig. S5: Observed (dots), calculated (line) and difference curve (bottom) of the XRD diffraction pattern of the *MA1000* ceramic measured at room temperature. The tick marks represent the reflections of the rhombohedral *R*3*m* phase. The planes indicated in the brackets correspond to the equivalent cubic phase reflections. **Inset:** Interatomic distances in the coordination sphere (< 3.2 Å) of Pb, Sc/Nb and O atomic positions obtained from the PSN structure refinement.

Table S2: Refined structural parameters for *MA1000* ceramics at RT in the space group *R*3m with *a* = 5.7694 (1) Å and *c* = 7.0864 (1) Å (Z = 3). Reliability factors: Robs = 1.76 %, Rwall = 1.76 %, Rp = 6.11 % and GoF = 1.12.

Atom	Wickoff position	Occ.	*x*	*y*	*z*	U_{iso}
Pb	3a	1	0	0	0.5	0.0303(6)
Sc	3a	0.5	0	0	0.0286(8)	0.0016(12)
Nb	3a	0.5	0	0	0.0286(8)	0.0016(12)
O	9b	1	0.8312(15)	0.1688(15)	0.213(2)	0.016(4)

The interatomic distances in the coordination spheres of Pb, Sc/Nb and O obtained from the PSN structure correspond well to the values of the ionic radii of the elements as given by Shannon [S9], *i.e.* r(Pb^{2+}[12]) = 1.49 Å, r(Nb^{5+}[6]) = 0.64 Å, r(Sc^{3+}[6]) = 0.745 Å, r(O^{2-}[8]) = 1.42 Å. In the O-O-O angles, a small tilting of the octahedral network occurs. A and B-site cations are displaced along the {111} direction of the cubic phase, which was previously observed by Malibert *et al*. using the neutron diffraction [S5]. Note however, that the displacement of the B-site cations is much larger, with the short / long distances of 1.95 Å / 2.13 Å instead of 2.02 Å / 2.06 Å. Furthermore, the theoretical density of 7.94 g/cm^3 was calculated using the unit cell parameters, obtained from the XRD pattern (Fig. S5).

E) Raman spectra of MA- and SS-derived PSN ceramics

Raman spectra were obtained with a LabRAM microprobe system (ISA/Jobin-Yvon/Horiba, Villeneuve d'Ascq, France) using a 532.02 nm Nd:YAG solid state laser as the excitation source. Surfaces of the sintered pellets were prepared by polishing with a 1 µm diamond paste. The laser light was focused on the sample surface at a long working distance 100x (N.A.=0.8) objective lens (LMPlan FI, Olympus, Japan); effective laser power at the sample surface was set to 3 mW. The spectra were collected in the true backscattering geometry with the aid of a Peltier-cooled charged coupled device camera. No significant influence of the different thermal treatment and/or processing on the ordering is evident from the Raman spectra, which is likely due to the higher sensitivity of Raman spectra to the defect population than to B-site ordering in these materials [S10].

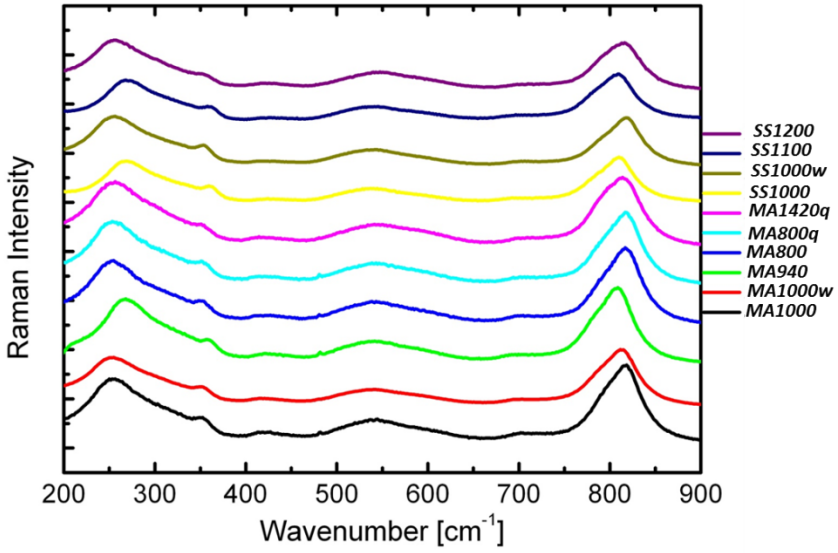

Fig. S6: Room-temperature Raman spectra of the PSN ceramics exposed to different thermal treatments.

F) Polarization vs electric field of MA-derived ceramics

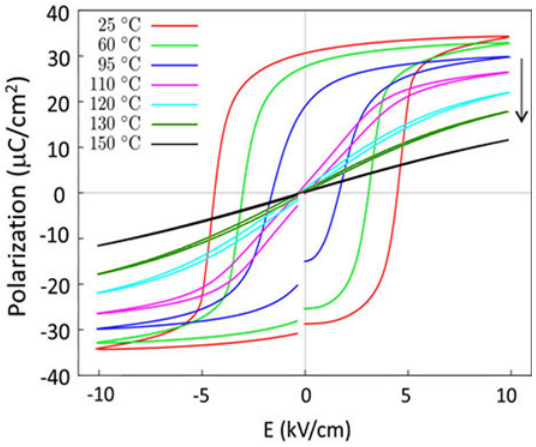

Fig. S7: *P-E* hysteresis loop vs. *T* for the *MA1000* ceramics at the maximum field of 1 kV/mm. The arrow indicates the increase in the temperature.

References

[S1] Perrin, C.; Menguy, N.; Bidault, O.; Zahra, C. Y.; Zahra, A. M.; Caranoni, C.; Hilczer, B.; Stepanov, A. Influence of B-site chemical ordering on the dielectric response of the $Pb(Sc_{1/2}Nb_{1/2})O_3$relaxor. *J. Phys.: Condens. Matter* **2001**, *13*, 10231-10245.

[S2] Chu, F.; Reaney, I. M.; Setter, N. Spontaneous (zero-field) relaxor-to-ferroelectric-phase transition in disordered $Pb(Sc_{1/2}Nb_{1/2})O_3$. *J. Appl. Phys.* **1995**, *77*, 1671-1676.

[S3] Zhu, M.; Chen, C.; Tang, J.; Hou, Y.; Wang, H.; Yan, H.; Zhang, W.; Chen, J.; Zhang, W.; Effects of ordering degree on the dielectric and ferroelectric behaviors of relaxor ferroelectric $Pb(Sc_{1/2}Nb_{1/2})O_3$ ceramics, *J. Appl. Phys.* **2008**, *103*, 084124 1-6.

[S4] Stenger, C. G. F.; Burggraaf, A. J. Order-disorder reactions in the ferroelectric perovskites $Pb(Sc_{0.5}Nb_{0.5})O_3$ and $Pb(Sc_{0.5}Ta_{0.5})O_3$, Kinetics of the Ordering Process. *Phys. State. Sol.* **1980**, *61*, 275-285.

[S5] Malibert, C; Dkhil, B; Kiat, J. M; Durand, D; Berar, J. F.; Spasojevic-de Bire A. Order and disorder in the relaxor ferroelectric perovskite $Pb(Sc_{1/2}Nb_{1/2})O_3$ (PSN): comparison with simple perovskite $BaTiO_3$ and $PbTiO_3$. *J. Phys.: Condens. Metter* **1997**, *9*, 7485-7500.

[S6] Yasuda, N.; Fujita, K. Effect of hydrostatic pressure on ferroelectric phase transition of lead scandium niobate. *Ferroelectrics* **1990**, *106*, 275-280.

[S7] Szafranski M., Hilczer A., Nawrocik W.; J. Phys.: Condens. Matter 16 (2004) 7025.

[S8] Kingery W. D., Bowen H. K., Uhlmann D. R., Introduction to Ceramics, John Wiley & Sons Inc., 1976, pp. 489

[S9] Shannon, R. D. Revised Effective Ionic Radii and Systematic Studies of Interatomic Distances in Halides and Chalcogenides, *Acta Cryst. A* **1976**, 32, 751.

[S10] Mihailova, B.; Gospodinov, M.; Guttler, B.; Petrova, D.; Stosch, R.; Bismayer, U. Ferroic nanoclusters in relaxors: the effect of oxygen vacancies. *J. Phys.: Condens. Matter* **2007**, *19*, 246220 1-10.